PCP
PLANT & CELL PHYSIOLOGY

Cyt $c_{6\text{-}3}$: A New Isoform of Photosynthetic Cyt c_6 Exclusive to Heterocyst-Forming Cyanobacteria

Alejandro Torrado, Ana Valladares, Leonor Puerto-Galán, Manuel Hervás, José A. Navarro and Fernando P. Molina-Heredia*

Instituto de Bioquímica Vegetal y Fotosíntesis, Universidad de Sevilla & CSIC, Américo Vespucio 49, 41092 Sevilla, Spain
*Corresponding author: E-mail, publio@us.es; Fax, +34-954-460-165.
(Received June 20, 2016; Accepted October 21, 2016)

Regular Paper

All known cyanobacteria contain Cyt c_6, a small soluble electron carrier protein whose main function is to transfer electrons from the Cyt b_6f complex to PSI, although it is also involved in respiration. We have previously described a second isoform of this protein, the Cyt c_6-like, whose function remains unknown. Here we describe a third isoform of Cyt c_6 (here called Cyt$c_{6\text{-}3}$), which is only found in heterocyst-forming filamentous cyanobacteria. Cyt $c_{6\text{-}3}$ is expressed in vegetative cells but is specifically repressed in heterocysts cells under diazotrophic growth conditions. Although there is a close structural similarity between Cyt $c_{6\text{-}3}$ and Cyt c_6 related to the general protein folding, Cyt $c_{6\text{-}3}$ presents differential electrostatic surface features as compared with Cyt c_6, its expression is not copper dependent and has a low reactivity towards PSI. According to the different expression pattern, functional reactivity and structural properties, Cyt $c_{6\text{-}3}$ has to play an as yet to be defined regulatory role related to heterocyst differentiation.

Keywords: Cyanobacteria • Cyt c_6 • Cyt $c_{6\text{-}3}$ • Cyt c_6-like • Heterocysts • *Nostoc* sp. PCC 7119 • PSI • Photosynthetic electron transfer chain • Plastocyanin • Respiratory electron transfer chain.

Abbreviations: Cox, cytochrome *c* oxidase; E_m, midpoint redox potential; $E_{m,7}$, midpoint redox potential at pH 7; GFP, green fluorescent protein; k_{bim}, second-order rate constant; k_{inf}, second-order rate constant extrapolated to infinite ionic strength; k_{obs}, observed pseudo-first-order rate constant; MALDI-TOF, matrix-assisted laser desorption ionization-time of flight; ORF, open reading frame; Pc, plastocyanin; p*I*, isoelectric point; qPCR, quantittive PCR. The nucleotide sequence reported in this paper has been submitted to EMBL with accession numbers HG316543.

Introduction

Cyt c_6 is a well-known soluble electron carrier between the two membrane-embedded Cyt b_6f and PSI complexes in oxygenic photosynthesis. It is present in all known cyanobacteria and in most green algae (Schmetterer 1994, Ki 2005). However, duing evolution from cyanobacteria to higher plants, Cyt c_6 has been replaced by plastocyanin (Pc) (Hervás et al. 2003). Actually both proteins are present in most cyanobacteria, where Cyt c_6 substitutes for Pc under copper deficiency conditions (Hervás et al. 2003). On the other hand, some green algae lack Cyt c_6 and in higher plants only Pc acts as the electron donor to PSI (Molina-Heredia et al. 2003, Weigel et al. 2003).

Cyanobacteria are the unique group of prokaryotic organisms capable of carrying out an oxygenic photosynthesis similar to that performed by plants (Blankenship 1992). They have a photosynthetic apparatus with two photosystems located in thylakoid membranes similar to those found in higher plant chloroplasts, of which cyanobacteria represent the phylogenetic ancestor. However, whereas in photosynthetic eukaryotes the respiratory and the photosynthetic electron transport chains are located in different cell organelles, in cyanobacteria both chains are located in the same membrane system, and thus they share some components (plastoquinone, Pc or Cyt c_6, and the Cyt b_6f complex). Consequently, in these prokaryotic organisms Cyt c_6 and Pc alternatively transport electrons from the Cyt b_6f complex not only to PSI but also to respiratory cytochrome *c* oxidases (Coxs) (Peschek 1999, Navarro et al. 2005). Moreover, although the cyanobacterial cytoplasmic membrane does not contain a functional photosynthetic electron transport chain, it holds a second respiratory chain (Schmetterer 1994). As nitrogen source, cyanobacteria can use nitrate, nitrite and ammonium, although some strains can use urea, amino acids or atmospheric nitrogen (Luque and Forchhammer 2008). In the latter case, under conditions of absence of combined nitrogen, some strains differentiate specialized cells called heterocysts. The dinitrogen fixation process is performed in these cells in order to separate it spatially from photosynthesis. This prevents the irreversible inactivation of nitrogenase by molecular oxygen (Wolk 1982, Fay 1992). In fact, the respiratory activity is higher in heterocysts than in vegetative cells in order to decrease O_2 concentration (Murray and Wolk 1989).

In cyanobacteria, along with its well-established role in photosynthesis and respiration (Kerfeld and Krogmann 1998, Kerfeld et al. 1999, Peschek 1999), Cyt c_6 has also been proposed to be involved in anoxygenic photosynthesis, in which Cyt c_6 could transport electrons from quinones to sulfoferric clusters during anaerobic oxidation of sulfur (Klatt et al. 2015). However, it remains unclear whether all these processes involve one or several isoforms of Cyt c_6 (Ki 2005). In numerous cyanobacteria, at least two genes that could encode two Cyt c_6 isoforms have been found (Ki 2005, Bialek et al. 2008, Reyes-Sosa

Plant Cell Physiol. 58(2): 256–265 (2017) doi:10.1093/pcp/pcw184, Advance Access publication on 25 October 2016, available online at www.pcp.oxfordjournals.org

et al. 2011). One of these isoforms is the genuine *petJ* gene, which encodes Cyt c_6, and the other one encodes a Cyt c_6-like protein (herein after Cyt $c_{6\text{-}2}$), which cannot oxidize the Cyt b_6f complex but can reduce, although with low efficiency, PSI (Reyes-Sosa et al. 2011). Also, Bialek et al. (2008) previously described two well-defined groups of cyanobacterial Cyt $c_{6\text{-}2}$ proteins, Cyt c_{6B} and Cyt c_{6C}, that do not appear to be present simultaneously in the same cyanobacterium (Ki 2005). The Cyt $c_{6\text{-}3}$ from *Nostoc* falls into the Cyt c_{6C} group. The presence of isogenes opens the door to the possibility that each one could perform a different metabolic function within a cyanobacterium.

To our knowledge, here we described and biochemically characterized for the first time a third isoform of Cyt c_6, here called Cyt $c_{6\text{-}3}$, which is only present in heterocyst-forming (filamentous) cyanobacteria. This protein cannot donate electrons efficiently to PSI, as Cyt c_6 and Pc do. Cyt $c_{6\text{-}3}$ is specifically repressed in heterocysts under diazotrophic conditions, and its expression is not copper regulated. The particular expression pattern of Cyt $c_{6\text{-}3}$ in heterocysts and vegetative cells may suggest a possible regulatory role related to heterocyst differentiation.

Results and Discussion

Cloning and sequencing of *Nostoc* Cyt $c_{6\text{-}3}$

On the basis of the known sequences of Cyt c_6, we searched in the CyanoBase (Kazusa DNA Research Institute) for genes encoding proteins homologous to this metalloprotein. In addition to the *petJ* Cyt c_6 gene, we found genes coding for Cyt $c_{6\text{-}2}$ (formerly Cyt c_6-like protein), Cyt c_M and for a fourth type of class I Cyt *c* homologous to Cyt c_6 which has not yet been described. Further search with BLASTP against major sequence databases (GenBank, EMBL and DDBJ) showed that this new Cyt *c* (here called Cyt $c_{6\text{-}3}$) is present only in the cyanobacterial families *Stigonematales* and *Nostocaceae*; specifically in the genera *Anabaena*, *Nostoc*, *Cylindrospermum*, *Fischerella*, *Calothrix* and *Cylindrospermopsis*, all encompassed in heterocyst-forming filamentous cyanobacteria. A Cyt $c_{6\text{-}3}$ sequence was also found in the genus *Raphidiopsis*, a filamentous cyanobacterium that is deemed to have lost the capacity to differentiate heterocysts (Mohamed 2007).

Using the sequence of Cyt $c_{6\text{-}3}$ from *Anabaena variabilis* (Ava_2744) as template, a couple of oligonucleotides outside the open reading frame (ORF) were designed, in order to clone the homologous gene from *Nostoc* sp. PCC 7119 by PCR amplification. We have chosen this strain because it has been intensively used in functional studies of both photosynthetic and respiratory electron transport chains. In order to avoid amplification of undesired DNA regions, a first PCR cycle using an annealing temperature of 43°C was critical, with the following cycles being carried out at 46°C. In these conditions, only one band was amplified (not shown). The PCR product was purified, ligated into pGEM-T cloning vector, subcloned in pBluescript II SK(+), thus generating the expression vector pEAC63-WT, and sequenced. The determined sequence of the *petJ-3* gene from *Nostoc* sp. PCC 7119 (EMBL accession No. HG316543) showed 97% identity with that from *A. variabilis*.

Sequence analysis

Fig. 1 shows the sequence alignment of the three isoforms of Cyt c_6 present in *Nostoc* sp. PCC 7119. Like Cyt c_6 and Cyt $c_{6\text{-}2}$, Cyt $c_{6\text{-}3}$ has a typical transit peptide to the periplasmic space/thylakoid lumen of 25 amino acids. This transit peptide consists of three well-defined regions: a positively charged N-terminal region, a central hydrophobic region and a C-terminal end comprising the consensus motif AxA, a specific cleavage site for peptidases. The cellular localization of Cyt $c_{6\text{-}3}$ is a key point when assessing its physiological role. In this context, the close similarity between the transit peptides of the three proteins (Fig. 1) suggests that they could, in fact, be located in the same cellular compartment.

It has been previously reported that the presence of a glutamine at position 50 (*Nostoc* Cyt c_6 numbering) in the sequence of a protein belonging to the Cyt c_6 family makes its redox potential approximately 100 mV higher that if this position is occupied by any other residue (Worral et al. 2007). Cyt $c_{6\text{-}3}$, as well as Cyt c_6 ($E_{m,7}$ = +335 mV), possess an equivalent glutamine in this location (positions 50 in Cyt c_6, and 54 in Cyt $c_{6\text{-}3}$; Fig. 1). However, this amino acid is absent in Cyt $c_{6\text{-}2}$ (replaced by isoleucine; Fig. 1), whose $E_{m,7}$ is +199 mV (see below). In addition, in *c*-type Cyts, the heme group is covalently attached to the polypeptide chain through the CxxCH motif, in which the histidine is one of the two axial ligands to the heme iron. In the *Nostoc* Cyt $c_{6\text{-}3}$ the complete sequence is CASCH, which is identical to that of Cyt c_6 (Fig. 1). Interestingly, in both Cyt $c_{6\text{-}2}$ and Cyt c_M (whose $E_{m,7}$ are about 150 mV lower than that of Cyt c_6), the sequence motif is CAGCH.

Cyt $c_{6\text{-}3}$ presents a 55% and 41% identity, and 68% and 56% homology, with Cyts c_6 and $c_{6\text{-}2}$, respectively, the identity and homology among Cyts c_6 and $c_{6\text{-}2}$ being 53% and 72%, respectively. However, Cyt $c_{6\text{-}3}$ contains two additional regions that are not present in Cyt c_6 or Cyt $c_{6\text{-}2}$, an internal region (LKYL) and five additional amino acids at the C-terminus (NLEKE) (Fig. 1).

Cyt c_6 interacts with PSI and Cyt *f*—in the Cyt b_6f complex—using two specific regions (Molina-Heredia et al. 1999, Díaz-Moreno et al. 2005). The first one is a hydrophobic surface, located around the area through which the heme group is exposed to solvent (residues I9, S11, N13, L24, V25 and K29), which provides a contact surface for the electron transfer. The second one is a charged area (residues A57, M58, A60, F61, K62, R64, L65 and K66), responsible for driving long-distance electrostatic interactions with PSI and Cyt b_6f complexes (Díaz-Moreno et al. 2005, De la Rosa et al. 2006). As shown in Fig. 1, most of these residues are conserved in both Cyt $c_{6\text{-}2}$ and Cyt $c_{6\text{-}3}$. In fact, Cyt $c_{6\text{-}2}$ is able to interact with PSI, although with an efficiency significantly lower than Cyt c_6 (Reyes-Sosa et al. 2011). Therefore, the presence of these two conserved regions in Cyt $c_{6\text{-}3}$ might also indicate that this protein could interact with Cyt b_6f or PSI and/or with Cox. However, the arginine residue at position 64 of Cyt c_6 (position 68 in Cyt $c_{6\text{-}3}$), strictly conserved in all cyanobacteria and which is

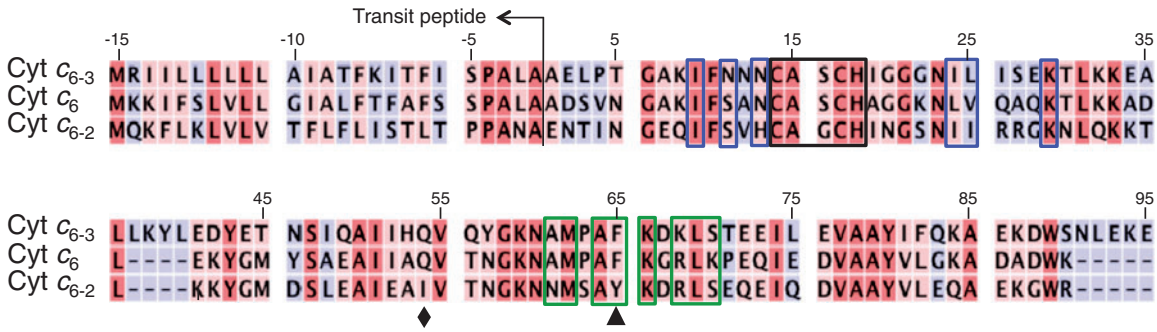

Fig. 1 Alignment of amino acid sequences of pre-Cyts c_6, $c_{6\text{-}2}$ and $c_{6\text{-}3}$ from *Nostoc* sp. PCC 7119. The arrow points to the transit peptides. Identical regions are shaded in red, similar regions in pink and non-similar regions in blue. The surface residues from Cyt c_6 involved in hydrophobic or electrostatic interactions with PSI are boxed in blue and green, respectively. Also, the heme-binding motifs are boxed in black. The rhombus points to the glutamine residue at position 50 in Cyt c_6 and 54 in Cyt $c_{6\text{-}3}$ that modulates the redox potential in the Cyt *c* protein family (see text). The triangle points to Tyr61 from Cyt $c_{6\text{-}2}$, conserved in all Cyt c_6-like proteins.

necessary for the efficient interaction with PSI (Molina-Heredia et al. 1999), although conserved in Cyt $c_{6\text{-}2}$ (Reyes-Sosa et al. 2011), is replaced in Cyt $c_{6\text{-}3}$ for a lysine residue. G63 and K66 (G67 and K70 in Cyt $c_{6\text{-}3}$) positions in the electrostatic area of Cyt c_6 are also replaced by aspartic and serine groups, respectively, in Cyt $c_{6\text{-}2}$ and Cyt $c_{6\text{-}3}$ (**Fig. 1**). Conversely, it has been described that in Cyt c_6 position 61 (65 in Cyt $c_{6\text{-}3}$) is always occupied by phenylalanine or tryptophan residues. Thus, a phenylalanine appears at this position in both *Nostoc* Cyt c_6 and Cyt $c_{6\text{-}3}$, whereas in Cyt $c_{6\text{-}2}$ this residue is a tyrosine (Bialek et al. 2008).

In order to elucidate the evolutionary relationships of Cyt $c_{6\text{-}3}$, we have compared the amino acid sequences of Cyt $c_{6\text{-}3}$ from different cyanobacteria with those of the six other soluble monoheme Cyts with hisidine–methionine axial metal co-ordination from photosynthetic organisms: Cyt c_6 (cyanobacteria), Cyt $c_{6\text{-}2}$ (cyanobacteria), Cyt c_M (cyanobacteria), Cyt c_2 (anoxygenic bacteria), Cyt c_{6A} (higher plants and green algae chloroplasts) and respiratory Cyt *c* (algal and plant mitochondria) (**Fig. 2**). As previously indicated, Cyt $c_{6\text{-}3}$ appears only in heterocyst-forming filamentous cyanobacteria and, as seen in **Fig. 2**, constitutes, by itself, a separate clade more related to Cyt c_6 than to Cyt $c_{6\text{-}2}$ or other photosynthetic Cyts.

Purification and physico-chemical characterization of *Nostoc* Cyt $c_{6\text{-}3}$

Cyt $c_{6\text{-}3}$ from *Nostoc* sp. PCC 7119 was expressed in *Escherichia coli* and purified as described in the Materials and Methods. Around 20 mg of Cyt $c_{6\text{-}3}$ were extracted from the periplasmic fraction of an *E. coli* 30 liter cell culture, and 10 mg of pure Cyt $c_{6\text{-}3}$, with an A_{275}/A_{552} absorbance ratio of 1.17 for the reduced protein, were finally obtained. As the Cyt $c_{6\text{-}3}$ has a transit peptide to the thylakoid lumen/periplasmic space (see above), the recombinant protein was expressed in the periplasmic space of *E. coli*. Sequencing of the N-terminus and MALDI-TOF (matrix-assisted laser desorption ionization-time of flight) analysis confirmed that recombinant Cyt $c_{6\text{-}3}$ was correctly processed in *E. coli* cells (not shown, and see **Fig. 1**).

Fig. 3 shows the UV/visible absorption spectra of purified *Nostoc* Cyt $c_{6\text{-}3}$. Cyt $c_{6\text{-}3}$ presents typical spectroscopic features of *c*-type Cyts and similar to those of *Nostoc* Cyt c_6 and Cyt $c_{6\text{-}2}$ (Molina-Heredia et al. 1998, Reyes-Sosa et al. 2011). In the reduced state, *Nostoc* Cyt $c_{6\text{-}3}$ exhibits characteristic absorbance maxima at 552 (α), 522 (β), 416 (γ, or Soret), 319 (δ) and 275 nm (protein). Upon oxidation with ammonium persulfate, the α and β peaks are replaced by a broader band with a maximum at 528 nm, the Soret band shifts to 410 m, the δ band disappears, and a new band appears with a maximum at 358 nm (**Fig. 3**). Also, the extinction coefficient of Cyt $c_{6\text{-}3}$ at 552 nm was determined to be 24.8 $mM^{-1}\,cm^{-1}$ for the reduced protein, whereas the differential extinction coefficient, reduced minus oxidized, was 16.6 $mM^{-1}\,cm^{-1}$ (not shown).

The isoelectric point (p*I*) of Cyt $c_{6\text{-}3}$ was also determined (not shown). It should be borne in mind that the p*I* from Cyt c_6, and its functional counterpart Pc, presents a huge variation from one organism to another, but they are very similar within the same organism (De la Rosa et al. 2006, Hervás and Navarro 2011). Thus, in *Nostoc*, both proteins are basic, with a p*I* of 9.0 and 8.8, respectively (Molina-Heredia et al. 1998). The p*I* from *Nostoc* Cyt $c_{6\text{-}2}$, which is not a functional homolog of Cyt c_6, is 8.0 (Reyes-Sosa et al. 2011). On the other hand, the p*I* from *Nostoc* $c_{6\text{-}3}$ is 5.2 (not shown), thus being significantly different from that of Cyt c_6 and $c_{6\text{-}2}$.

The $E_{m,7}$ of *Nostoc* Cyt $c_{6\text{-}3}$ is +300 mV (**Table 1**), about 35 mV lower than those from Cyts c_6 and *f* (Molina-Heredia et al. 1998, Albarrán et al. 2005), and 100 mV higher than that from Cyt $c_{6\text{-}2}$ (Reyes-Sosa et al. 2011). As mentioned previously, these data are consistent with the presence of a glutamine at position 54 in Cyts c_6 and $c_{6\text{-}3}$, that is absent in Cyt $c_{6\text{-}2}$. At pH 4.0, closer to the physiological pH inside the thylakoidal lumen under illumination (Kramer et al. 1999), the E_m from Cyt $c_{6\text{-}2}$ and Cyt $c_{6\text{-}3}$ increases to +30 and +40 mV, respectively (**Table 1**), and thus both Cyts c_6 and $c_{6\text{-}3}$ become isopotential (**Table 1**). Although it was not possible to determine the E_m at pH 4.0 from the recombinant soluble fragment of *Nostoc* Cyt *f*, because at this pH the protein became denaturalized, just from a thermodynamic point of view it is plausible that Cyt $c_{6\text{-}3}$ would be able to accept electrons from Cyt *f*.

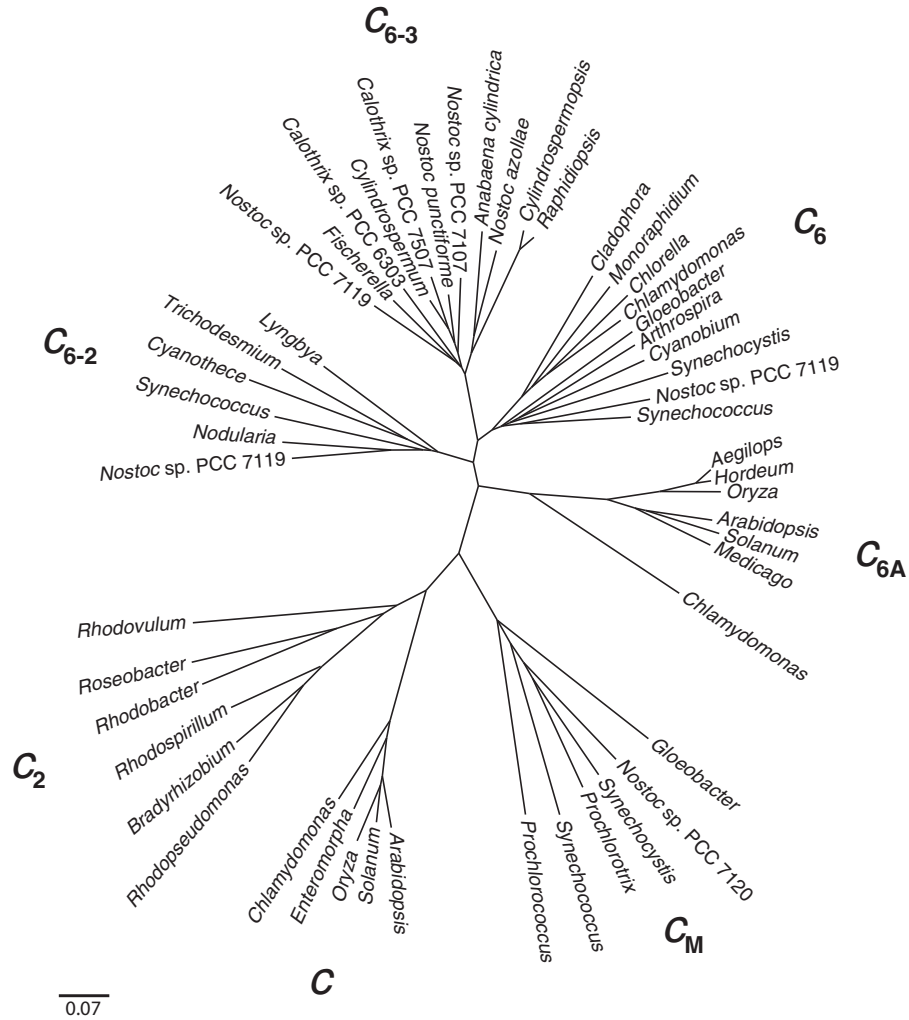

Fig. 2 Phylogenetic tree of histidine–methionine Fe-co-ordinated soluble Cyts from photosynthetic organisms. The tree was constructed by protein maximum likelihood with PROTML (MOLPHY) (Adachi and Hasegawa 1992). The following sequences were aligned: Cyt $c_{6\text{-}3}$ ($c_{6\text{-}3}$) of *Anabaena cylindrica* PCC 7122 (GenBank gi 440681468), *Calothrix* sp. PCC 6303 (GenBank gi 428297476), *Calothrix* sp. PCC 7507 (GenBank gi 427719567), *Cylindrospermopsis raciborskii* (GenBank gi WP_006276584.1), *Cylindrospermum stagnale* PCC 7417 (GenBank gi 434404902), *Fischerella* sp. JSC-11 (GenBank gi 497072149), *Nostoc azollae* 0708 (GenBank gi 298490297), *Nostoc punctiforme* PCC 73102 (GenBank gi 186683068), *Nostoc* sp. PCC 7107 (GenBank gi 427710665), *Nostoc* sp. PCC 7119 (TrEMBL HG316543), *Raphidiopsis brookii* (GenBank gi WP_009344415.1); Cyt c_6 (c_6) of *Arthrospira platensis* NIES-39 (GenBank gi YP_005072220.1), *Chlamydomonas reinhardtii* (GenBank gi 117924), *Chlorella vulgaris* (GenBank gi 30578153), *Cladophora glomerata* (GenBank gi 24636293), *Cyanobium* sp. PCC 7001 (GenBank gi 493967399), *Gloeobacter violaceus* (GenBank gi 37521549), *Monoraphidium braunii* (GenBank gi 729268), *Nostoc* sp. PCC 7119 (EMBL AJ002361), *Synechococcus elongatus* (GenBank gi 25014058), *Synechocystis* sp. PCC 6803 (EMBL P46445); Cyt c_{6A} (c_{6A}) of *Aegilops speltoides* (GenBank gi 11222607), *Arabidopsis thaliana* (GenBank gi 9783643), *Chlamydomonas reinhardtii* (C_820065), *Hordeum vulgaris* (GenBank gi 16311393), *Medicago trunculata* (GenBank gi 11610049), *Oryza sativa* (GenBank gi 8955747), *Solanum tuberosum* (GenBank gi 13615108); Cyt c_M (c_M) of *Gloeobacter violaceus* (GenBank gi 37522351), *Nostoc* sp. PCC 7120 (gi 17228860), *Prochlorococcus marinus* subsp. *pastoris* CCMP1378 (GenBank gi 33861613), *Prochlorothrix hollandica* (GenBank gi 4098525), *Synechococcus* sp. WH 8102 (GenBank gi 33865254), *Synechocystis* sp. PCC 6803 (GenBank gi 16330764); respiratory Cyt *c* (*c*) of *Arabidopsis thaliana* (GenBank gi 16177), *Chlamydomonas reinhardtii* (GenBank gi 322374), *Enteromorpha intestinalis* (GenBank gi 65520), *Oryza sativa* (GenBank gi 2394300), *Solanum tuberosum* (GenBank gi 65506); Cyt c_2 (c_2) of *Bradyrhizobium* sp. ORS278 (TrEMBL Q8VUB4), *Rhodobacter capsulatus* (TrEMBL P00094), *Rhodopseudomonas palustris* (TrEMBL Q8GI80), *Rhodospirillum centenum* (TrEMBL P81153), *Rhodovulum sulfidophilum* (TrEMBL Q93I63), *Roseobacter denitrificans* (TrEMBL P07625); and Cyt $c_{6\text{-}2}$ ($c_{6\text{-}2}$) of *Cyanothece* sp. CCY0110 (GenBank gi 126660190), *Lyngbya* sp. PCC 8106 (GenBank gi 119484682), *Nodularia spumigena* CCY9414 (GenBank gi 119509989), *Nostoc* sp. PCC 7119 (EMBL AM902496), *Synechococcus elongatus* PCC 6301 (GenBank gi 56751577) and *Trichodesmium erythraeum* IMS101 (GenBank gi 113478003). Branch lengths reflect the estimated number of substitutions/site.

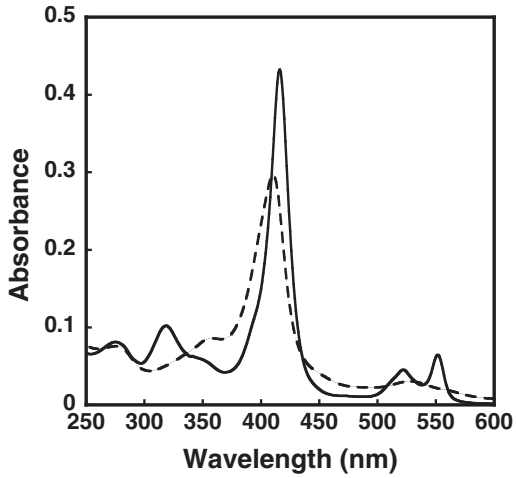

Fig. 3 UV/visible absorption spectra of the purified Cyt $c_{6\text{-}3}$ from *Nostoc* sp. PCC 7119 expressed in *E. coli* cells, both in its native reduced state (continuous line) and after oxidation by a small excess of ammonium persulfate (dashed line).

Structural modeling

To analyze the interaction of Cyt $c_{6\text{-}3}$ with possible partners it is not only the p*I* of the protein, which indicates the whole molecule charge responsible for the long-distance electrostatic interactions, that is important, but it is also essential to take into account the surface distribution of electrostatic charges and hydrophobic patches, responsible for short-distance orientations. For this reason, we have modeled the 3D structure of Cyt $c_{6\text{-}3}$ and compared it with the structure of Cyt c_6 (**Fig. 4**). As previously mentioned, *Nostoc* Cyt c_6 has two areas of interaction with PSI or Cyt b_6f. In turn, Cyt $c_{6\text{-}3}$ has two short insertions that are not present in Cyt c_6. A mid four-residue insertion leads to an extension in the central α-helix that could be related to the interaction with PSI, whereas a final insertion presents an undefined secondary structure. Although both insertions are difficult to be modeled accurately, and thus the quality of the model could influence the fine distribution of charges on the surface of the molecule, the global charge distribution of the model can give us relevant information about the electrostatic properties of the protein. The three Cyt isoforms conserve the hydrophobic region around the area where the heme group is accessible to the solvent and involved in the electron transfer reaction, but not the electrostatic surface involved in the formation of the transient electrostatic complex with either PSI or Cyt *f* (Molina-Heredia et al. 1999, Molina-Heredia et al. 2001, Crowley et al. 2002, Díaz-Moreno et al. 2005).

Functional analysis of the interaction of Cyt $c_{6\text{-}3}$ with PSI

To check a possible function of Cyt $c_{6\text{-}3}$ in the photosynthetic electron transfer chain, we have performed a laser flash-induced kinetic analysis of PSI reduction by this protein. **Table 1** shows the value for the second-order rate constant (k_{bim}) of PSI reduction by Cyt $c_{6\text{-}3}$, inferred from the slope of the linear plot of the observed pseudo-first-order rate constant (k_{obs}) vs. the protein concentration (not shown). For a comparative analysis, the previously determined values corresponding to *Nostoc* Cyt c_6, Cyt $c_{6\text{-}2}$ and Pc are also presented (**Table 1**). The k_{bim} for PSI reduction is approximately 75 and 50 times lower for Cyt $c_{6\text{-}3}$ than for Cyt c_6 and Pc, respectively, and 20 times lower than for Cyt $c_{6\text{-}2}$. The ionic strength dependence of the reaction rates provides further evidence for the lack of reactivity of Cyt $c_{6\text{-}3}$ towards PSI; whereas for both Cyt c_6 and Pc the rate constants decrease with salt concentration (Hervás et al. 1995, Molina-Heredia et al. 1998) and are basically independent of ionic strength with Cyt $c_{6\text{-}2}$ (Reyes-Sosa et al. 2011), they slightly increase with Cyt $c_{6\text{-}3}$ (data not shown). However, the k_{bim} value extrapolated at infinite ionic strength (k_{inf}) for Cyt $c_{6\text{-}3}$ still remains noticeable diminished as compared with the other three proteins (**Table 1**). These findings indicate that Cyt $c_{6\text{-}3}$ does not react efficiently with PSI, even at physiological ionic strengths.

Cyt $c_{6\text{-}3}$ detection and cell localization

The low fluorescence emitted by the AT4 strain, expressing sf-GFP (superfolding variant of green fluorescent protein) fused to the C-terminal region of Cyt $c_{6\text{-}3}$ indicated a very low expression of Cyt $c_{6\text{-}3}$ under the conditions tested (not shown). Thus, to confirm that the AT4 strain expresses the fusion protein, a Western blot detection assay, using anti-GFP antibodies, was performed. Cyt $c_{6\text{-}3}$ immunodetection with antibodies against this protein was not possible, as these antibodies also recognized Cyt c_6 (not shown) and the reaction with this latter protein (with a similar molecular weight) impeded the visualization of Cyt $c_{6\text{-}3}$. As shows in **Fig. 5**, the Cyt $c_{6\text{-}3}$–sf-GFP fusion protein was expressed in the AT4 strain under standard conditions in the presence of nitrate, as a band (absent in the wild-type strain) with the molecular weight corresponding to the fusion protein was clearly detected. This finding demonstrates, unequivocally, that Cyt $c_{6\text{-}3}$ is expressed in *Nostoc*. **Fig. 5** also indicated that, when *Nostoc* is growing under diazotrophic conditions, the expression of Cyt $c_{6\text{-}3}$ decreases significantly.

These results were further confirmed by immunofluorescence assays on the AT9 strain, bearing the *petJ-3* sequence with a 6×His tag in the C-terminal region. Although the immunoassays are less informative than confocal microscopy, thus losing information on the subcellular localization, this technique allows a higher amplification of the signal and the detection of proteins with low expression levels. **Fig. 6** confirms that Cyt $c_{6\text{-}3}$ is expressed in cells grown with nitrate as nitrogen source (**Fig. 6B**) and that if cells are grown in diazotrophic conditions the expression is repressed (**Fig. 6C**). **Fig. 6C** also shows a filament containing one heterocyst. In this case, no fluorescence differences are observed between vegetative and heterocyst cells, due to the low fluorescence intensity, similar to the background fluorescence (**Fig. 6A, C**).

Finally, it is well established that Cyt c_6 and Pc expression is inversely regulated by copper, the expression of Cyt c_6 being strongly repressed by the presence of the metal and that of Pc being repressed in its absence (Bovy et al. 1992). For this reason, we have studied the effect of the presence or absence of copper

Table 1 Midpoint redox potential (E_m) at pH 4 and 7, and kinetic parameters for *Nostoc* PSI reduction by Cyt c_6, Cyt $c_{6\text{-}2}$ and Cyt $c_{6\text{-}3}$

Protein	E_m, pH 4 (mV)	E_m, pH 7 (mV)	k_{bim} (M^{-1} s^{-1}) × 10^{-7}	k_{inf} (M^{-1} s^{-1}) × 10^{-6}
Cyt c_6	+340	+335[a]	12.1[a]	11.4[a]
Cyt $c_{6\text{-}2}$	+230	+199[b]	3.2[b]	4.0[b]
Cyt $c_{6\text{-}3}$	+343	+300	0.16	2.5

[a] Data from Molina-Heredia et al. (1998).
[b] Data from Reyes-Sosa et al. (2011).

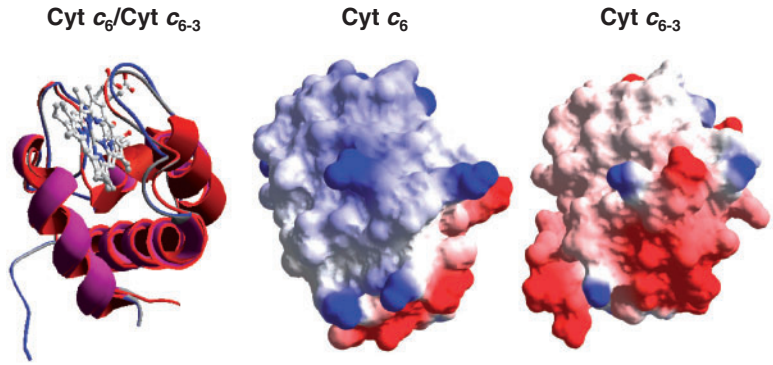

Fig. 4 Backbone alignment representation of Cyt c_6 (red) and Cyt $c_{6\text{-}3}$ (blue) from *Nostoc* sp. PCC 7119, and surface electrostatic potential distribution. Both Cyts are represented in the same orientation, with their respective electrostatic-charged 'east' faces (site 2) in front and the 'north' hydrophobic poles (site 1) at the top. Simulations of surface electrostatic potential distribution were performed assuming an ionic strength of 50 mM at pH 7.0. Positively and negatively charged regions are depicted in blue and red colors, respectively.

in the expression of the *petJ* and *petJ-3* genes. **Supplementary Fig. S1** shows the results of quantitative PCR (qPCR) analysis with RNA isolated from wild-type cells grown with nitrate and in the presence or absence of copper. The obtained results show that *petJ* (Cyt c_6) transcription is copper repressed, as expected, but *petJ-3* (Cyt $c_{6\text{-}3}$) expression is copper independent.

In vivo GFP report of the Cyt $c_{6\text{-}3}$ promoter activity

To obtain more insights into the regulation of the *petJ-3* gene expression in the different cell types of *Nostoc* grown in diazotrophic conditions, a strain expressing GFP under the control of the promoter region of the *petJ-3* gene was constructed. In this strain, the *gfp* gene was fused to the first four triplets of the *petJ-3* gene, thus eliminating the transit peptide to the periplasmic space/thylakoid lumen.

As shown in **Fig. 7**, under nitrogen-limiting conditions, fluorescence from GFP was observed in both vegetative cells and heterocysts, but the expression in vegetative cells was about 30% higher than in heterocysts. In order to analyze whether the *petJ-3* promoter is induced transiently or not during heterocyst differentiation, fluorescence from GFP was monitored at different times after combined nitrogen deprivation, a condition that triggers heterocyst differentiation. No significant changes were observed in the expression pattern with increasing time, indicating that the differences in expression in heterocysts and vegetative cells are not just transiently induced by nitrogen limitation.

Cyt c_6 is a small soluble heme protein, present in all known cyanobacteria (Schmetterer 1994, Ki 2005), whose principal function is to transfer electrons from the Cyt b_6f complex to PSI in the photosynthetic electron transfer chain. In most cyanobacteria, the copper protein Pc functionally substitutes Cyt c_6 in the presence of copper in the medium (Hervás et al. 2003). In addition, a second form of Cyt c_6 Cyt $c_{6\text{-}2}$ is also present (Ki 2005, Bialek et al. 2008, Reyes-Sosa et al. 2011). At present, the possible function of Cyt $c_{6\text{-}2}$ remains unknown.

Many researchers have speculated about the possible existence of a third electron donor to PSI to explain some aspects of the respiratory and photosynthetic processes that remain unknown. For example, it has been described that *Synechocystis* sp. PCC 6803, which only presents one isoform of Cyt c_6, can grow photoautotrophically in the absence of both Cyt c_6 and Pc (Ardelean et al. 2002). Here we describe a third form of Cyt c_6, Cyt $c_{6\text{-}3}$.

Cyt $c_{6\text{-}3}$ only appears in filamentous cyanobacteria able to develop heterocysts, and this suggests a function related either to heterocysts metabolism or to the differentiation process. Cyt $c_{6\text{-}3}$ does not substitute Cyt c_6 and Pc in photosynthetic electron transfer chains, as it cannot reduce PSI, and the detected in vivo protein levels are too low to be an efficient replacement for the abundant canonical soluble electron donors.

In the presence of combined nitrogen, Cyt $c_{6\text{-}3}$ is homogeneously expressed in all the cells of the filament. The protein seems to be expressed in the thylakoid lumen and in the periplasmic space, although the fluorescence signal is too low to confirm this with absolute certainty. Under nitrogen starvation, the expression of Cyt $c_{6\text{-}3}$ is partially repressed in vegetative

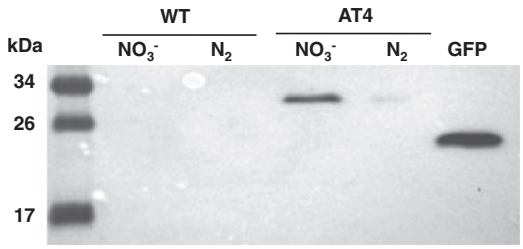

Fig. 5 Detection of Cyt $c_{6\text{-}3}$ protein by Western blot analysis of *Nostoc* sp. PCC 7119 wild-type and AT4 strains, expressing a Cyt $c_{6\text{-}3}$–GFP fusion protein, grown with combined nitrogen (NO_3^-) or in diazotrophic conditions (N_2), and by using and anti-GFP antibody.

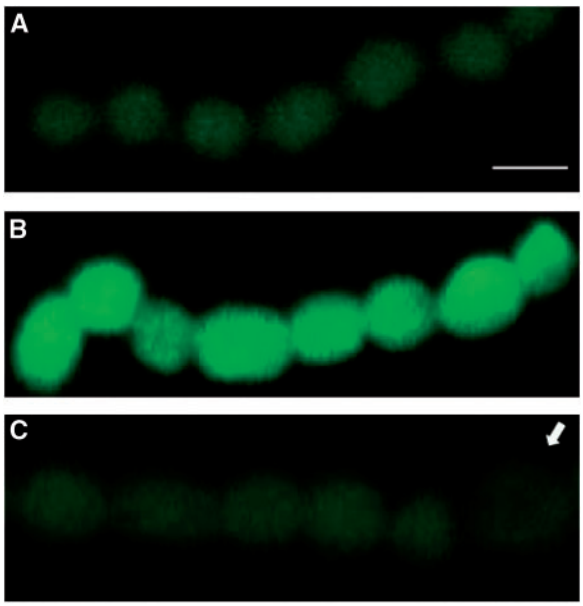

Fig. 6 Immunofluorescence localization of Cyt $c_{6\text{-}3}$ in *Nostoc* sp. PCC 7119 wild type (A) and in the AT9 strain (B, C), expressing Cyt $c_{6\text{-}3}$ His-tagged in BG11 (A, B) or BG110 (C). Filaments were incubated for 48 h with the indicated nitrogen source, prepared for immunofluorescence analysis with anti-6×His antibody and visualized by fluorescence microscopy. Size bar = 6 μm; magnification was the same for all micrographs. Arrow points to a heterocyst.

cells, but such repression is practically complete in heterocysts. Thus, it is possible that Cyt $c_{6\text{-}3}$ could play an as yet to be defined regulatory role, related to heterocyst differentiation.

Materials and Methods

Bacterial strains and plasmids

The genomic DNA used in this work was isolated from an axenic culture of the filamentous heterocyst-forming cyanobacteria *Nostoc* sp. PCC 7119, formerly *Anabaena* (Adolph and Haselkorn 1971). *Escherichia coli* DH5α (Bethesda Research Laboratories) was used for cloning and general DNA manipulations. *Escherichia coli* MC1061 (Casadaban and Cohen 1980) was used for the heterologous expression of Cyt $c_{6\text{-}3}$. The pBluescript II SK(+) plasmid (Stratagene) was used to construct the plasmid pEAC63-WT, for overexpression of the *Nostoc* Cyt $c_{6\text{-}3}$ (this work). The plasmid pEC86 (Arslan et al. 1998), which encodes the *E. coli* genes required for Cyt *c* maturation, was used to enhance the expression of Cyt $c_{6\text{-}3}$ in *E. coli*.

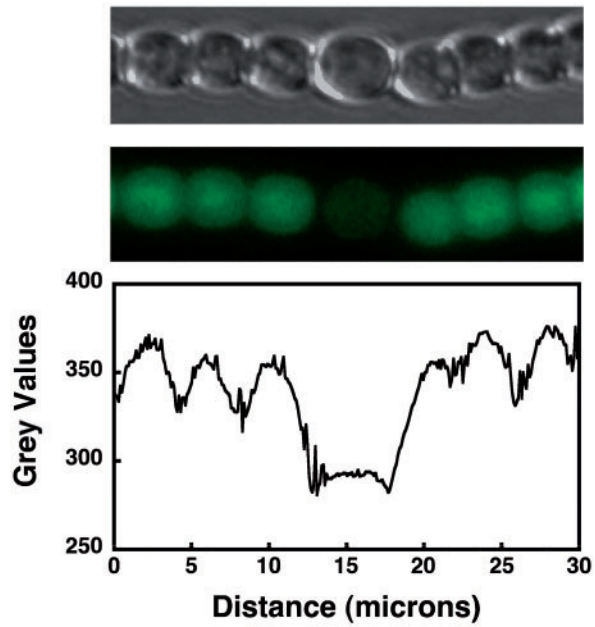

Fig. 7 Filaments of strain AT1 (*petJ-3-gfp*) incubated for 24 h in medium lacking combined nitrogen and visualized by bright field (upper) or fluorescence confocal microscopy (middle). Lower: quantification of GFP fluorescence from each cell along the filament. Average background fluorescence from wild-type cells (lacking GFP) was subtracted. The central cell is a heterocyst. Gray values represent the absolute amount of fluorescence in the cells.

Cloning and sequencing of the *petJ-3* gene from *Nostoc* sp. PCC 7119

The forward (GCATAAGTTGCTAGAG) and reverse (GCTACACGAATTAAGC TTG) primers, used to amplify the region containing the *petJ-3* gene from the genomic DNA of *Nostoc* sp. PCC 7119 by PCR, were deduced from the ORF Ava_2744, which putatively encodes a Cyt *c* class I (*GI:75908956*) in *A. variabilis* ATCC 29413 (http://genome.microbedb.jp/cyanobase) (Fujisawa et al. 2014). To clone this gene selectively in phase with the *lac* promoter of the pGEM-T and pBluescript II SK(+) cloning vectors, the restriction site *Hin*dIII was added to the 3′ end of the gene. The resulting PCR product was cloned using the pGEM-T vector system (Promega). To ensure that the sequences did not contain any mutations introduced by PCR, two independent amplifications were carried out and two independent clones of each were sequenced separately. The DNA Sequencing Service from the Spanish National Cancer Research Centre (CNIO, Madrid) carried out the nucleotide sequence analysis. The resulting ORF was afterwards subcloned in pBluescript II SK(+), generating the plasmid pEAC63-WT. This plasmid was used for the expression of the *petJ-3* gene under the control of the *lac* promoter. Other molecular biology protocols used were standard.

Multiple alignment and phylogenetic analysis

The sequence homology between the Cyt $c_{6\text{-}3}$ and other related photosynthetic Cyt *c*-type proteins was analyzed using the BLASTP network service of the National Center for Biotechnology Information (www.ncbi.nlm.nih.gov). Signal peptides were analyzed with the SignalP 3.0 Server (Emanuelsson et al. 2007). Multiple alignments of protein sequences were carried out using the CLUSTAL W (version 2.0.3) program (Thompson et al. 1994). The phylogenetic tree was created by protein maximum likelihood with PROTML (MOLPHY) (Adachi and Hasegawa 1992).

Strain construction

To construct the AT1, bearing GFP under the control of *petJ-3* promoter, and AT2/AT4 strains, bearing the *petJ/petJ-3-sf-gfp* translational fusion of *Nostoc* sp.

PCC 7119, DNA was transferred to *Nostoc* sp. PCC 7119 by triparental mating with *E. coli* promoted by the conjugative plasmid pRL443, as described by Elhai and Wolk (1988). For the AT1 strain, the DNA fragment from the *petJ-3* promoter region was amplified by PCR using primer pairs AT1-F/AT1-R (**Supplementary Table S1**), including *Hin*dIII and *Eco*RV sites, and cloned into the conjugation plasmid pCSAM137 (bearing the *gfp* gene; Flores et al. 2007), generating the pCAT1 plasmid. In this construct, the *gfp* gene is translationally fused to the tree first codons of the *petJ-3* gene. For AT2 and AT4 strains, DNA fragments of the genes containing promoter regions and the entire genes were amplified by PCR using primer pairs AT2-F/AT2-R and AT4-F/AT4-R (**Supplementary Table S1**), respectively, including *Hin*dIII and *Bsa*I sites, and cloned into the pCSAL34 plasmid (bearing the *sf-gfp-mut2* gene; Burnat et al. 2014). After that, the construction was subcloned into the conjugation plasmid pCSV3 (Olmedo-Verd et al. 2006), in the *Kpn*I restriction site, producing the pCAT2 and pCAT4 plasmids, respectively. The genetic structure of selected clones from each mating was tested by PCR with total DNA from the clone, using the forward primers of each construct and reverse primer *gfp4* to check the presence of the GFP and sf-GFP fusions. The accumulation of GFP was analysed by laser confocal microscopy, using a Leica HCX-Plan-APO ×63/1.4 NA objective and a Leica TCS SP2 microscope, as described by Olmedo-Verd et al. (2006).

To construct the AT9 strain of *Nostoc* sp. PCC 7119 for immunofluorescence analysis, bearing the *petJ-3* sequence with a 6×His tag in the C-terminal region, DNA was transferred to *Nostoc* sp. PCC 7119 by triparental mating as described before. The plasmid containing the *petJ-3-6×His* fusion was developed by Genecust (Distribio), using pBluescript II SK (+) (Stratagene) as template, including a *Kpn*I restriction site, and was cloned into pCSV3, producing the pCAT9 plasmid.

Structural modeling

The structure of Cyt $c_{6\text{-}3}$ from *Nostoc* sp. PCC 7119 was modeled using the program Phyre[2] (http://www.sbg.bio.ic.ac.uk/phyre2) (Kelley and Sternberg 2009). The surface electrostatic potential of this protein was modeled using the Swiss-Pdb Viewer (Guex and Peitsch 1997) as described previously (Reyes-Sosa et al. 2011). The quality of the modeled structures was tested using the PROCHECK program (Laskowski et al. 1993).

Protein expression and purification procedures

Escherichia coli MC1061 cells co-transformed with both pEAC63-WT and pEC86 plasmids were grown in standard LB medium supplemented with 100 μg ampicillin ml^{-1} and 20 μg chloramphenicol ml^{-1}. Cells from 30 liters of culture were collected by centrifugation and resuspended in 225 ml of 10 mM Tris–HCl buffer (pH 7.5). The periplasmic fraction was extracted by freeze–thaw cycles (Eftekhar and Schiller 1994) and extensively dialyzed against the same buffer. Subsequently, it was applied to a DEAE Sepharose column equilibrated with the same buffer. Cyt $c_{6\text{-}3}$ was eluted with a 0–0.4 M NaCl linear gradient. The fractions containing Cyt $c_{6\text{-}3}$ were pooled, concentrated and further purified by gel filtration using a Sephacryl S-200 HR column (GE Healthcare Life Sciences) in 10 mM Tris–HCl buffer (pH 7.5) supplemented with 100 mM NaCl. An A_{275}/A_{552} absorbance ratio of 1.17 was obtained for pure protein in its reduced state. Final pure protein fractions were pooled, concentrated and extensively dialyzed against 10 mM Tris–HCl, pH 7.5. Protein concentration was determined spectrophotometrically using an absorption coefficient of 24.8 $mM^{-1}cm^{-1}$ at 552 nm for the reduced protein (this work). Recombinant *Nostoc* Cyt c_6, Pc, Cyt $c_{6\text{-}2}$ and Cyt *f* were expressed and purified as previously described (Molina-Heredia et al. 1999, Molina-Heredia et al. 2001, Albarrán et al. 2005, Reyes-Sosa et al. 2011). PSI particles were isolated from *Nostoc* cells by β-dodecyl maltoside solubilization as described previously (Molina-Heredia et al. 1999). The P700 content in PSI samples was calculated from the photo-induced absorbance changes at 820 nm using the absorption coefficient of 6.5 $mM^{-1}cm^{-1}$ determined by Mathis and Sétif (1981). The Chl concentration was determined according to Arnon (1949).

Analytical methods

The extinction coefficient of *Nostoc* sp. PCC 7119 Cyt $c_{6\text{-}3}$ at 552 nm (24.8 $mM^{-1}cm^{-1}$) was determined using the pyridine hemochrome method (Appleby 1969). In order to check that the expressed protein was correctly processed, the N-terminus was sequenced in a Procise TM 494 Protein Sequencer (Applied Biosystems). Redox titrations were performed as described previously (Molina-Heredia et al. 1998). The p*I* was determined by electrofocusing (Robertson et al. 1987), with a mixture of carrier ampholytes from Bio-Rad, pH range 3–10; the standard proteins used were those of the Sigma isoelectric focusing calibration kit for a pH range of 6.8–9.3. Molecular weights were determined by MALDI-TOF analysis (Bruker Daltonics).

RNA isolation and real-time quantitative PCR

Cells from cultures grown with the indicated nitrogen sources, either in the presence or absence of copper, and bubbled with air supplemented with 1% CO_2, were collected by filtration (nitrocellulose filter 0.45 μm) and washed in RNase-free TE buffer (10 mM Tris–HCl, pH 7.5, and 1 mM EDTA). Pelleted cells were reduced to dust with a mortar after freezing in liquid nitrogen. Total RNA was extracted using 1 ml of TRIsure reagent (BIOLINE) according to the manufacturer's instructions. Afterwards, RNA was extracted with phenol and chloroform/isoamyl alcohol (24 : 1), precipitated with absolute ethanol and washed with 70% ethanol. Finally, RNA was resuspended in 25 μl of RNase-free water. cDNA synthesis was performed with 1 μg of total RNA using the QuantiTect reverse Transcription kit (QIAGEN) according to the manufacturer's instructions. Real-time qPCR was performed using the SensiFAST SYBR & Fluorescein kit (BIOLINE) and the IQ5 real-time PCR detection system (BIO-RAD). A standard thermal profile (95°C, 3 min; 40 cycles at 95°C for 10 s, and 60°C for 30 s) was used for all reactions. Oligonucleotides used for qPCR analyses are described in **Supplementary Table S1**. Expression levels were normalized using *rnpB* as a housekeeping gene.

Immunofluorescence of Cyt $c_{6\text{-}3}$

Immunofluorescence of Cyt $c_{6\text{-}3}$ was performed as described by Ramos-León et al. (2015) with minor variations. The primary antibody used was rabbit anti-6×His (Sigma) diluted 1 : 500 in phosphate-buffered saline (PBS; 26 mM NaCl, 540 μM KCl, 800 μM Na_2HPO_4, 352 μM KH_2PO_4) supplemented with 0.05 % Tween-20 (PBS-T) and 5% milk powder.

Protein sample and Western blotting

Cells from *Nostoc* sp. PCC 7119 cultures grown in BG11 (containing $NaNO_3$) or in $BG11_0$ (without combined nitrogen) (Rippka et al. 1979) were collected by centrifugation (5,000 × *g*, 5 min) and resuspended in Resuspension buffer (50 mM HEPES-NaOH pH 7.5, 30 mM $CaCl_2$, 800 mM D-sorbitol and 1 mM ε-amino-*n*-caproic acid). Afterwards, 250 mg of 500 μm diameter glass beads (Biospec products) were added, mixed by vortex during 1 min and incubated on ice for 1 min more. This process was repeated seven times, and then 200 μl of Resuspension buffer were added, centrifuged (1,500 × *g*, 1 min, 4 °C) and the supernatant was collected. The pellet was resuspended in 400 μl of Resuspension buffer and centrifuged (1,500 × *g*, 1 min, 4°C). The supernatant was unified and centrifuged (3,000 × *g*, 3 min, 4°C) to clean the sample. The protein content of the supernatant was quantified by the Lowry method (Lowry 1951); 20 μg of the sample was loaded into a 1 % SDS–polyacrylamide gel and run for 90 min at 150 V. After that, the gel was transferred to a nitrocellulose 0.45 μM pore size membrane (Amersham Protran) with a Trans-Blotting turbo system (BioRad) for 30 min (25 V and 1 A). The membrane was then incubated for 1 h at room temperature with blocking buffer (PBS-T + 5% milk powder), and then incubated overnight at 4°C with primary antibody [anti-GFP 1 : 2,000 (Santa Cruz Biotechnology)] diluted in PBS-T. The membrane was washed three times during 5 min in PBS-T and incubated for 1 h at room temperature with secondary antibody [anti-rabbit IgG peroxidase (Sigma)] diluted 1 : 10,000 in PBS-T. The membrane was washed three more times with PBS-T and signal was visualized with an Immobilon Western kit (Millipore).

Laser flash absorption spectroscopy

Kinetics of flash-induced absorbance changes associated with PSI photooxidation and further re-reduction by Cyt $c_{6\text{-}3}$ were followed at 830 nm as described previously (Bernal-Bayard et al. 2013). The standard reaction mixture

contained, in a final volume of 0.2 ml, 20 mM Tricine-KOH buffer, pH 7.5, 10 mM $MgCl_2$, 0.03% β-dodecyl maltoside, an amount of PSI particles equivalent to 0.35 mg Chl ml^{-1}, 0.1 mM methyl viologen, 2 mM sodium ascorbate and Cyt $c_{6\text{-}3}$ at increasing concentrations. All the experiments were performed at 22°C in a 1 mm pathlength cuvette. Kinetic data collection, analyses and values for the observed pseudo-first-order rate constants (k_{obs}), the second-order rate constant (k_{bim}) and the second-order rate constant extrapolated to infinite ionic strength (k_{inf}) for PSI reduction were estimated according to formalisms previously described (Hervás et al. 2005, Hervás and Navarro 2011). Typically, the estimated error in the k_{obs} determination was ≤10%, based on the reproducibility and signal-to-noise ratios.

Supplementary data

Supplementary data are available at PCP online.

Funding

This work has been supported by the Fundación de Investigación de la Universidad de Sevilla (FIUS, Spain) [grant FIUS05710000]; the Ministerio de Economía y Competitividad, Spain [grants BIO2012-35271 and BIO2015-64169-P]; the Andalusian Government [PAIDI BIO-022] and FEDER.

Disclosures

The authors have no conflicts of interest to declare.

Acknowledgments

We acknowledge A. Herrero and E. Flores for helpful discussions and critically reading the manuscript, and A. Orea and R. Rodríguez for technical assistance with confocal microscopy and mass spectrometry, respectively.

References

Adachi. J. and Hasegawa, M. (1992) MOLPHY version 2.3: programs for molecular phylogenetics based on maximum likelihood. *Comput. Sci. Monogr.* 28: 1–77.

Adolph, K.W. and Haselkorn, R. (1971) Isolation and characterization of a virus infecting the blue-green alga *Nostoc muscorum*. *Virology* 46: 200–208.

Albarrán, C., Navarro, J.A., Molina-Heredia, F.P., Murdoch, P.S., De la Rosa, M.A. and Hervás, M. (2005) Laser flash-induced kinetic analysis of cytochrome *f* oxidation by wild-type and mutant plastocyanin from the cyanobacterium *Nostoc* sp. PCC 7119. *Biochemistry* 44: 11601–11607.

Appleby, C.A. (1969) Electron transport systems of *Rhizobium japonicum*. II. Rhizobium haemoglobin, cytochromes and oxidases in free-living (cultured) cells. *Biochim. Biophys. Acta* 172: 88–105.

Ardelean, I., Matthijs, H.C., Havaux, M., Jose, F. and Jeanjean, R. (2002) Unexpected changes in photosystem I function in a cytochrome c_6-deficient mutant of the cyanobacterium *Synechocystis* PCC 6803. *FEMS Microbiol Lett.* 213: 113–119.

Arnon, D.I. (1949) Copper enzymes in isolated chloroplasts. Polyphenoloxidase in *Beta vulgaris*. *Plant Physiol.* 24: 1–15.

Arslan, E., Schulz, H., Zufferey, R., Künzler, P. and Thöny-Meyer, L. (1998) Overproduction of the *Bradyrhizobium japonicum c*-type cytochrome subunits of the cbb3 oxidase in *Escherichia coli*. *Biochem. Biophys. Res. Commun.* 251: 744–747.

Bernal-Bayard, P., Molina-Heredia, F.P., Hervás, M. and Navarro, J.A. (2013) Photosystem I reduction in diatoms: as complex as the green lineage systems but less efficient. *Biochemistry* 52: 8687–8695.

Bialek, W., Nelson, M., Tamiola, K., Kallas, T. and Szczepaniak, A. (2008) Deeply branching c_6-like cytochromes of cyanobacteria. *Biochemistry* 47: 5515–5522.

Blankenship, R.E. (1992) Origin and early evolution of photosynthesis. *Photosynth. Res.* 33: 91–111.

Bovy, A., de Vrieze, G., Borrias, M. and Weisbeek, P. (1992) Transcriptional regulation of the plastocyanin and cytochrome c_{553} genes from the cyanobacterium *Anabaena* species PCC 7937. *Mol. Microbiol.* 6: 1507–1513.

Burnat, M., Herrero, A. and Flores, E. (2014) Compartmentalized cyanophycin metabolism in the diazotrophic filaments of a heterocyst-forming cyanobacterium. *Proc. Natl. Acad. Sci. USA* 111: 3823–3828.

Casadaban, M.J. and Cohen, S.N. (1980) Analysis of gene control signals by DNA fusion and cloning in *Escherichia coli*. *J. Mol. Biol.* 138: 179–207.

Crowley, P.B., Díaz-Quintana, A., Molina-Heredia, F.P., Nieto, P.M., Sutter, M., Haehnel, W., et al. (2002) The interactions of cyanobacterial cytochrome c_6 and cytochrome *f*, characterized by NMR. *J. Biol. Chem.* 277: 48685–48689.

De la Rosa, M.A., Molina-Heredia, F.P., Hervás, M. and Navarro, J.A. (2006) Convergent evolution of cytochrome c_6 and plastocyanin. *In* Advances in Photosynthesis and Respiration. Edited by Goldbeck, J.H. pp. 683–694. Springer, Dordrecht.

Díaz-Moreno, I., Díaz-Quintana, A., Molina-Heredia, F.P., Nieto, P.M., Hansson, O., De la Rosa, M.A., et al. (2005) NMR analysis of the transient complex between membrane photosystem I and soluble cytochrome c_6. *J. Biol. Chem.* 280: 7925–7931.

Eftekhar, F. and Schiller, L.N. (1994) Partial purification and characterization of a mannuronan-specific alginate lyase from *Pseudomonas aeruginosa*. *Curr. Microbiol.* 29: 37–42.

Elhai, J. and Wolk, C.P. (1988) Conjugal transfer of DNA to cyanobacteria. *Methods Enzymol.* 167: 747–754.

Emanuelsson, O., Brunak, S., von Heijne, G. and Nielsen, H. (2007) Locating proteins in the cell using TargetP, SignalP and related tools. *Nat. Protoc.* 2: 953–971.

Fay, P. (1992) Oxygen relations of nitrogen fixation in cyanobacteria. *Microbiol. Rev.* 56: 340–373.

Flores, E., Pernil, R., Muro-Pastor, A.M., Mariscal, V., Maldener, I., Lechno-Yossef, S., et al. (2007) Septum-localized protein required for filament integrity and diazotrophy in the heterocyst-forming cyanobacterium *Anabaena* sp. strain PCC 7120. *J. Bacteriol.* 189: 3884–3890.

Fujisawa, T., Okamoto, S., Katayama, T., Nakao, M., Yoshimura, H., Kajiya-Kanegae, H., et al. (2014) CyanoBase and RhizoBase: databases of manually curated annotations for cyanobacterial and rhizobial genomes. *Nucleic Acids Res.* 42: D666–D670.

Guex, N. and Peitsch, M.C. (1997) SWISS-MODEL and the Swiss-PdbViewer: an environment for comparative protein modeling. *Electrophoresis* 18: 2714–2723.

Hervás, M. and Navarro, J.A. (2011) Effect of crowding on the electron transfer process from plastocyanin and cytochrome c_6 to photosystem I: a comparative study from cyanobacteria to green algae. *Photosynth. Res.* 107: 279–286.

Hervás, M., Díaz-Quintana, A., Kerfeld, C.A., Krogmann, D.W., De la Rosa, M.A. and Navarro, J.A. (2005) Cyanobacterial Photosystem I lacks specificity in its interaction with cytochrome c_6 electron donors. *Photosynth. Res.* 83: 329–333.

Hervás, M., Navarro, J.A. and De la Rosa, M.A. (2003) Electron transfer between membrane complexes and soluble proteins in photosynthesis. *Acc. Chem. Res.* 36: 798–805.

Hervás, M., Navarro, J.A., Díaz, A., Bottin, H. and De la Rosa, M.A. (1995) Laser-flash kinetic analysis of the fast electron transfer from plastocyanin and cytochrome c_6 to photosystem I. Experimental evidence on the evolution of the reaction mechanism. *Biochemistry* 34: 11321–11326.

Kelley, L.A. and Sternberg, M.J. (2009) Protein structure prediction on the Web: a case study using the Phyre server. *Nat. Protoc.* 4: 363–371.

Kerfeld, C.A. and Krogmann, D.W. (1998) Photosynthetic cytochromes *c* in cyanobacteria, algae, and plants. *Annu. Rev. Plant Physiol. Plant Mol. Biol.* 49: 397–425.

Kerfeld, C.A., Ho, K.K. and Krogmann, D.W. (1999) The cytochrome *c* of cyanobacteria. *In* The Prototrophic Prokaryotes. Edited by Peschek, G., Löffelhardt, W. and Schmetterer, G. pp. 259–268. Kluwer Academic/Plenum Publishers, New York.

Ki, H.K. (2005) Cytochrome c_6 genes in cyanobacteria and higher plants. *In* Handbook of Photosynthesis, 2nd edn. Edited by Pessarakli, M. pp. 286–297. CRC Press, Boca Raton, FL.

Klatt, J.M., Al-Najjar, M.A., Yilmaz, P., Lavik, G., de Beer, D. and Polerecky, L. (2015) Anoxygenic photosynthesis controls oxygenic photosynthesis in a cyanobacterium from a sulfidic spring. *Appl. Environ. Microbiol.* 81: 2025–2031.

Kramer, D.M., Sacksteder, C.A. and Cruz, J.A. (1999) How acidic is the lumen? *Photosynth. Res.* 60: 151–163.

Laskowski, R.A., McArthur, M.W., Moss, D.S. and Thornton, J.M. (1993) PROCHECK: a program to check the stereochemical quality of protein structure. *J. Appl. Crystallogr.* 26: 283–291.

Lowry, O.H., Rosenbrough, N.J., Farr, A. and Randall, R.J. (1951) Protein measurement with the Folin phenol reagent. *J. Biol. Chem.* 193: 265–75.

Luque, I. and Forchhammer, K. (2008) Nitrogen assimilation and C/N balance sensing. *In* The Cyanobacteria: Molecular Biology, Genomics and Evolution. Edited by Herrero, A. and Flores, E. pp. 335–385. Caister Academic Press, Norfolk, UK.

Mathis, P. and Sétif, P. (1981) Near infra-red absorption spectra of the chlorophyll a cations and triplet state in vitro and in vivo. *Isr. J. Chem.* 21: 316–320.

Mohamed, Z.A. (2007) First report of toxic *Cylindrospermopsis raciborskii* and *Raphidiopsis mediterranea* (Cyanoprokaryota) in Egyptian fresh waters. *FEMS Microbiol. Ecol.* 59: 749–761.

Molina-Heredia, F.P., Díaz-Quintana, A., Hervás, M., Navarro, J.A. and De la Rosa, M.A. (1999) Site-directed mutagenesis of cytochrome c_6 from *Anabaena* species PCC 7119. Identification of surface residues of the hemeprotein involved in photosystem I reduction. *J. Biol. Chem.* 274: 33565–33570.

Molina-Heredia, F.P., Hervás, M., Navarro, J.A. and De la Rosa, M.A. (1998) Cloning and correct expression in *Escherichia coli* of the *petE* and *petJ* genes respectively encoding plastocyanin and cytochrome c_6 from the cyanobacterium *Anabaena* sp. PCC 7119. *Biochem. Biophys. Res. Commun.* 243: 302–306.

Molina-Heredia, F.P., Hervás, M., Navarro, J.A. and De la Rosa, M.A. (2001) A single arginyl residue in plastocyanin and in cytochrome c_6 from the cyanobacterium *Anabaena* sp. PCC 7119 is required for efficient reduction of photosystem I. *J. Biol. Chem.* 276: 601–605.

Molina-Heredia, F.P., Wastl, J., Navarro, J.A., Bendall, D.S., Hervás, M., Howe, C.J., et al. (2003) Photosynthesis: a new function for an old cytochrome?. *Nature* 424: 33–34.

Murray, M.A. and Wolk, C.P. (1989) Evidence that the barrier to the penetration of oxygen into heterocysts depends of two layers of cell envelope. *Arch. Microbiol.* 151: 469–474.

Navarro, J.A., Durán, R.V., De la Rosa, M.A. and Hervás, M. (2005) Respiratory cytochrome *c* oxidase can be efficiently reduced by the photosynthetic redox proteins cytochrome c_6 and plastocyanin in cyanobacteria. *FEBS Lett.* 579: 3565–3568.

Olmedo-Verd, E., Muro-Pastor, A.M., Flores, E. and Herrero, A. (2006) Localized induction of the *ntcA* regulatory gene in developing heterocysts of *Anabaena* sp. strain PCC 7120. *J. Bacteriol.* 188: 6694–6699.

Peschek, G.A. (1999) Photosynthesis and respiration in cyanobacteria. Bioenergetic significance and molecular interactions. *In* The Phototrophic Prokaryotes. Edited by Peschek, G.A., Löffelhardt, W. and Schmetterer, G. pp. 201–209. Kluwer Academic/Plenum Publishers, New York.

Ramos-León, F., Mariscal, V., Frías, J.E., Flores, E. and Herrero, A. (2015) Divisome-dependent subcellular localization of cell–cell joining protein *SepJ* in the filamentous cyanobacterium *Anabaena*. *Mol. Microbiol.* 96: 566–580.

Reyes-Sosa, F.M., Gil-Martínez, J. and Molina-Heredia, F.P. (2011) Cytochrome c_6-like protein as a putative donor of electrons to photosystem I in the cyanobacterium *Nostoc* sp. PCC 7119. *Photosynth. Res.* 110: 61–72.

Rippka, R., Deruelles, J., Waterbury, J.B., Herdman, M. and Stanier, R.Y. (1979) Generic assignments, strain histories and properties of pure cultures of cyanobacteria. *J. Gen. Microbiol.* 111: 1–61.

Robertson, E.F., Dannelly, H.K., Malloy, P.J. and Reeves, H.C. (1987) Rapid isoelectric focusing in a vertical polyacrylamide minigel system. *Anal. Biochem.* 167: 290–294.

Schmetterer, G. (1994) Cyanobacterial respiration. *In* The Molecular Biology of Cyanobacteria. Edited by Bryant, D.A. pp. 409–435. Kluwer Academic Publishers, Dordrecht.

Thompson, J.D., Higgins, D.G. and Gibson, T.J. (1994) CLUSTAL W: improving the sensitivity of progressive multiple sequence alignment through sequence weighting, position-specific gap penalties and weight matrix choice. *Nucleic Acids Res.* 22: 4673–4680.

Weigel, M., Varotto, C., Pesaresi, P., Finazzi, G., Rappaport, F., Salamini, F., et al. (2003) Plastocyanin is indispensable for photosynthetic electron flow in *Arabidopsis thaliana*. *J. Biol. Chem.* 278: 31286–31289.

Wolk, C.P. (1982) Heterocysts. *In* The Biology of Cyanobacteria. Edited by Carr, B.A. pp. 359–386. Blackwell Scientific Publications, Oxford,.

Worrall, J.A., Schlarb-Ridley, B.G., Reda, T., Marcaida, M.J., Moorlen, R.J., Wastl, J., et al. (2007) Modulation of heme redox potential in the cytochrome c_6 family. *J. Amer. Chem. Soc.* 129: 9468–9475.